

Mössbauer study of $\text{Na}_{0.82}\text{CoO}_2$ (doped by 1% ^{57}Fe).

M. Pissas*, V. Psycharis, D. Stamopoulos, G. Papavassiliou, Y. Sanakis, A. Simopoulos
Institute of Materials Science, NCSR, Demokritos, 15310 Ag. Paraskevi, Athens, Greece
 (Dated: November 19, 2018)

We studied by Mössbauer spectroscopy the $\text{Na}_{0.82}\text{CoO}_2$ compound using 1% ^{57}Fe as a local probe which substitutes for the Co ions. Mössbauer spectra at $T = 300$ K revealed two sites which correspond to Fe^{3+} and Fe^{4+} . The existence of two distinct values of the quadrupole splitting instead of a continuous distribution should be related with the charge ordering of Co^{+3} , Co^{+4} ions and ion ordering of Na(1) and Na(2). Below $T = 10$ K part of the spectrum area, corresponding to Fe^{4+} and all of Fe^{3+} , displays broad magnetically split spectra arising either from short-range magnetic correlations or from slow electronic spin relaxation.

PACS numbers: 76.80.+y 75.20.-g, 75.20.Hr

Recently, it has been discovered¹ that H_2O intercalation in the Na_xCoO_2 compound induces superconductivity with $T_c \sim 5$ K, triggering a large research activity. Besides this remarkable discovery, the understanding of the magnetic properties of the triangular geometrically frustrated CoO_2 plane is a very important topic in strongly correlated electron systems. Novel types of magnetic transitions and ground states are expected due to the suppression of a long range magnetic ordering by the geometrical frustrations.

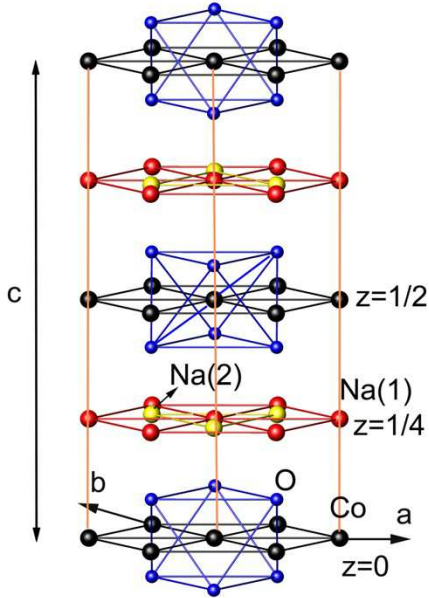


FIG. 1: Crystal structure of the $\text{Na}_{0.82}\text{CoO}_2$ compound.

In addition, this category of compounds has been used as cathodic material for solid state batteries² and thermoelectric devices.³ The basic characteristic of these compounds is the non-stoichiometry which permits reversible incorporation of foreign atoms in their lattice, without modification of the local configuration of the atoms or crystallographic structure. Depending on x , Na_xCoO_2 compound displays several crystal structures.⁴ The crystal structure is in general hexagonal, consisting of *edge-*

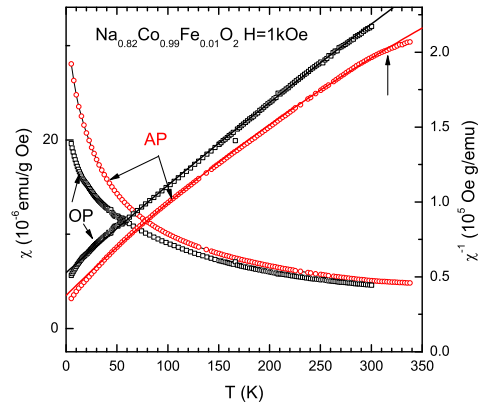


FIG. 2: Temperature variation of the mass susceptibility χ (left axis) and χ^{-1} (right axis), of the AP and OP $\text{Na}_{0.82}\text{CoO}_2$ samples. The symbols represent the experimental points, while the solid lines, are plots of the inverse susceptibility χ^{-1} using the parameters mentioned in the text. The vertical arrow shows the temperature where deviation from the linearity is observed.

sharing CoO_6 octahedra in between which the sodium ions are intercalated within a trigonal prismatic or octahedral environment. The CoO_2 forms a 2D hexagonal layer structure (see Fig. 1). Due to the deficiency at Na site $1-x$ holes are doped into the band insulating state of low spin Co^{3+} ($S = 0$, $3d^6$ in t_{2g} orbital). Alternatively, one can consider that the Na deficiency is equivalent with x electron doping in the triangular lattice consisting of Co^{4+} $S = 1/2$. Besides for the elucidation of the mechanism which is responsible for the superconductivity, there are still several open questions concerning the charge segregation^{5,6,7,8} in CoO_2 layers in the samples with $x \sim 3/4$, asking for further study. In the present paper we study the physical properties of the Na_xCoO_2 compound at a local level, using as local probe the iron impurity, which substitutes for the cobalt ions.

A sample with nominal composition $\text{Na}_{0.82}\text{Co}_{0.99}\text{Fe}_{0.01}\text{O}_2$ was prepared by solid state

reaction of Na_2CO_3 , Co_3O_4 and $^{57}\text{Fe}_2\text{O}_3$ at $T = 800^\circ\text{C}$ for 24h in air. Subsequently, the initial sample was separated into two parts at which we applied different heat treatment. The first part was additionally heated in air atmosphere at $T = 800^\circ\text{C}$, for 24 h. We call this sample AP. The second part was annealed at $T = 800^\circ\text{C}$ for 24 h in oxygen atmosphere and we call this OP sample. X-ray powder diffraction (XRD) data were collected with a D500 SIEMENS diffractometer, using $\text{CuK}\alpha$ radiation and a graphite crystal monochromator, from 4° to 100° in steps of 0.03° in 2Θ . The power conditions were set at 40KV/35mA. The aperture slit as well as the soller slit were set at 1° . The absorption Mössbauer spectra (MS) were recorded using a conventional constant acceleration spectrometer with a $^{57}\text{Co}(\text{Rh})$ source moving at room temperature, while the absorber was kept fixed in a variable temperature cryostat. The resolution was determined to be $\Gamma/2 = 0.12$ mm/sec using a thin $\alpha\text{-Fe}$ foil. DC magnetization measurements were performed in a SQUID magnetometer (Quantum Design). ^{23}Na NMR line shape measurements of the central transition ($-1/2 \rightarrow 1/2$) were performed on a home made spectrometer operating in external magnetic field $\mathcal{H} = 8$, Tesla. The spectra were obtained from the Fourier transform of half of the echo. The spin echo was generated with a two-pulse $\pi/2\text{-}\tau\text{-}\pi$ spin-echo pulse sequence.

Fig.2 shows the temperature variation of the mass magnetic susceptibility (χ) and the inverse magnetic susceptibility (χ^{-1}) for the AP and OP samples. The inverse magnetic susceptibility displays a nearly linear variation with temperature, implying a paramagnetic behavior with a small temperature independent magnetic susceptibility. Deviation from the Curie-Weiss equation was found below ~ 36 K and ~ 15 K for AP and OP samples respectively, suggesting that magnetic correlations take place below those temperatures. An additional deviation from the linearity of the χ^{-1} curve, was observed for the AP sample at $T \approx 315$ K (see arrow in Fig. 2) most probably being related with the $H1 - H2$ -structural transition.⁹ Thus, we fitted the experimental data for $36 < T < 315$ K for AP sample and for $T > 15$ K for OP sample, using a nonlinear least-square method, using the Curie-Weiss formula $\chi = C/(T - \Theta) + \chi_0$, where C is the Curie constant, Θ is Weiss temperature, and χ_0 the temperature independent susceptibility. The estimated from least-square fitting parameters are: $\Theta(\text{AP}) = -53(5)$ K, $\Theta(\text{OP}) = -86(1)$ K, $\mu_{\text{eff}}^2(\text{AP}) = 1.14\mu_{\text{B}}^2$, $\mu_{\text{eff}}^2(\text{OP}) = 1.21\mu_{\text{B}}^2$ and $\chi_0(\text{AP}) = 1.3(3) \times 10^{-6}$ emu/g Oe, $\chi_0(\text{OP}) = 4.5(4) \times 10^{-7}$ emu/g Oe for AP and OP samples, respectively. The negative value of Weiss temperature, for both samples, suggests that the spins interact predominantly antiferromagnetically. The observed effective magnetic moment μ_{eff} is given by the relationship $\mu_{\text{eff}}^2 = \sum_{i=1}^4 g_i^2 x_i S_i(S_i + 1)$, where $g_i = 2$ is the Landé factor, and x_i and S_i is the percentage and the spin of each individual ion i respectively. In the present case Co is present in the $\text{Co}^{3+}(S = 0)$ and Co^{4+}

($S = 1/2$) states. The Mössbauer spectroscopic studies to be presented below suggest that Fe is in $\text{Fe}^{3+}(S = \frac{5}{2})$ and $\text{Fe}^{4+}(S = 2)$ forms with a ratio 40/60. Taking this into consideration, the observed μ_{eff} can be accounted for by mixed valence configurations consisting of 37% Co^{4+} , ($S_1 = \frac{1}{2}$), 62% $\text{Co}^{+3}(S_2 = 0)$ for AP sample and 39% Co^{4+} , ($S_1 = \frac{1}{2}$), 60% $\text{Co}^{+3}(S_2 = 0)$ for OP sample. The estimated magnetic moments are in good agreement with those from other works.^{5,10,11,12}

The x-ray diffraction data at $T = 300$ K were analyzed using the Rietveld refinement method, with the FULLPROF suite of programs¹³, assuming the hexagonal $P6_3/mmc$ (no 194) space group for both samples. The crystal model used in the refinement is the so called H2-structure where, Co occupies the $2a(0,0,0)$ position, O the $4f(1/3,2/3,z)$, Na(1) the $2b(0,0,1/4)$ while for Na(2) we tested either $2d(2/3,1/3,1/4)$ or $2c(1/3,2/3,1/4)$ sites. The estimated unit cell parameters were $a = 2.8399(1)\text{\AA}$, $c = 10.8301(6)\text{\AA}$ for the AP sample and $a = 2.8382(1)\text{\AA}$, $c = 10.8572(3)\text{\AA}$ for the OP sample. Fig. 3 shows Rietveld plots for both AP and OP samples. From very initial refinement steps we ascertained that the Na(2) atoms exclusively occupy the $2d(2/3,1/3,1/4)$ site. That is, they do not "prefer" oxygen ions above and below (see Fig. 1). Let us discuss firstly the AP sample. Firstly, we would like to point out that our Rietveld refinement results for AP sample do not show evidence for two phase behavior at 300 K. After few refinement steps we achieved good agreement indexes. Looking on refinement results we found that both Na sites are partially occupied and display, large temperature factors $\sim 3\text{\AA}^2$, in agreement with the results of the Refs. 14,15. The intensity of the (101) Bragg peak is representative of the overall Na content. The refinement converge when 22% of Na(1) site is occupied and 51% of Na(2), giving an overall stoichiometry $\text{Na}_{0.73\pm 0.03}\text{CoO}_2$ for the AP sample. This stoichiometry is slightly lower than the nominal one. The lower Na content is possibly related with both the volatility of Na oxides and unreacted Na_2CO_3 , which amounted to a few per cent of the total. The large temperature factors of Na sites may imply that the Na(2) atom is not located exactly at $2d$ site. A common practice in overcoming this problem is to permit the x and y coordinates of Na(2) atoms to vary during the refinement as the $6h(2x,x,1/4)$, $x = 0.281(4)$, site imposes.¹⁶ Using this model the refinement converged at lower agreement indexes with more reasonable temperature factors. As far as the OP sample is concerned, the refinement gave similar results with the AP sample. However, close inspection of the high angle part of the (001) Bragg peaks revealed small shoulders (see the inset of the lower part of Fig. 3). These shoulders possibly originate from crystallites with lower c -axis length in comparison with the majority phase. Based on this, we employ a two phase refinement in agreement with Ref. 9 where their $\text{Na}_{0.75}\text{CoO}_2$ compound, (which prepared in oxygen atmosphere), below $T \approx 340$ K, displayed two-phase behavior. This model gave substantially better agreement

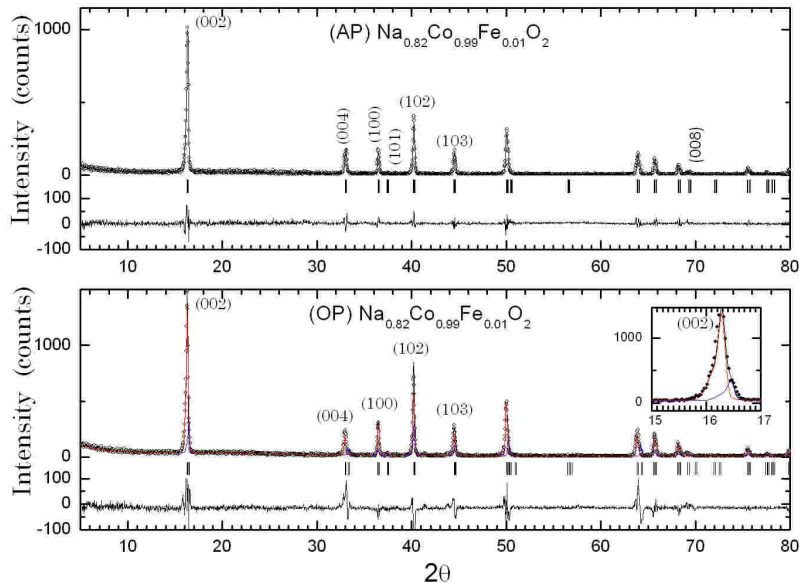


FIG. 3: Rietveld plots for AP and OP $\text{Na}_{0.82}\text{Co}_{0.99}\text{Fe}_{0.01}\text{O}_2$ samples. The observed data points are indicated by open circles, while the calculated and difference patterns are shown by solid lines. The positions of the reflections are indicated by vertical lines below the patterns. The inset shows a zoom of the (002) Bragg peak for the OP sample. The shoulder at the high angle place correspond to a second Na_xCoO_2 phase with slight lower c -axis.

indexes.

^{23}Na NMR spectra obtained at $T = 300, 175$ and 50 K are displayed in Fig. 4. The spectra seen in Fig. 4 concern the central part of the spectrum, corresponding to the $-\frac{1}{2} \rightarrow \frac{1}{2}$ transition, of our AP sample. The echo intensity, arising from the quadrupole wings of the transitions $\pm\frac{3}{2} \leftrightarrow \pm\frac{1}{2}$, was not observed, probably because our sample is polycrystalline. The spectrum, at 50 K comprises three peaks. The low-frequency line most probably arises from un-reacted Na and/or defect Na sites. The remaining doublet may tentatively be assigned into two Na sites, in agreement with crystal structure data. Using similar arguments like those of Ref. 6 we can claim that at low temperatures some kind of ordering in the two Na sites, occurs. At higher temperatures the thermal motion of Na^+ ions results in motional narrowing, causing a gradually merging of the two lines into a single line.^{6,10}

Mössbauer spectra were taken for both samples at temperatures between $T = 4.2$ K and $T = 300$ K. The paramagnetic and the magnetically split Mössbauer spectra at 300 K and 4.2 K are least-squares fitted with two and three components, respectively and the results are summarized in Table I. The spectra of the AP sample, at $T = 300$ K, consist of two components (see Fig. 5) with isomer shift (with respect to Fe metal at 300 K) of -0.06 mm/s and 0.38 mm/s respectively. Based on isomer shift values, the first component can be assigned either to low spin Fe^{2+} ($S = 0$) or to high spin Fe^{4+}

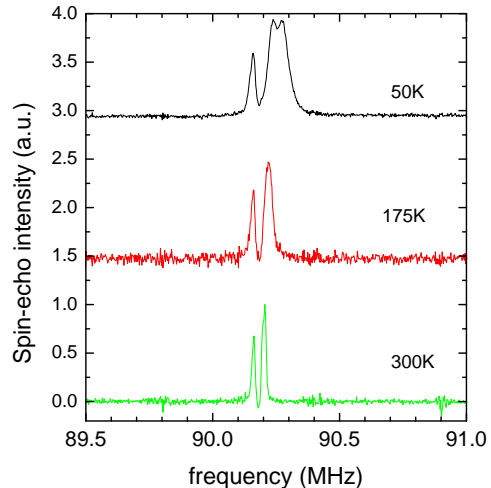


FIG. 4: ^{23}Na NMR spectra at $T = 50, 175$ and 300 K.

($S = 2$). The second component is probably high spin ferric ($S = 5/2$). Their spectra area ratio is 60% to 40%. This ratio remains constant down to 10 K indicating that they have similar Debye-Waller factors. Considering that the parent compound comprises Co^{3+} and Co^{4+} ions the site with small isomer shift is attributed to Fe^{4+} ($S = 2$). Our assignment will be made clearer below where we will discuss the magnetically split spec-

tra. According to our Rietveld results, the Na content is 0.73, implying a $\text{Co}^{4+}:\text{Co}^{3+} \approx 0.25 : 0.75$ and as a consequence, if iron follows the Co ions, we would expect a $\text{Fe}^{4+}:\text{Fe}^{3+} \approx 0.25 : 0.75$. The observed area ratio of the two components is different than the expected if we assume that the Fe impurities substitute for Co^{4+} and Co^{3+} in the lattice.

Regarding the quadrupole interaction we note that the Fe^{4+} component displays a small quadrupole splitting of ~ 0.18 mm/s and the Fe^{3+} a splitting of ~ 0.50 mm/s. Both components appear with narrow linewidths (0.15 mm/s for Fe^{4+} and 0.24 mm/s for Fe^{3+}). Interestingly, although the iron randomly substitutes the Co ions, the two iron sites, except for the different isomer shift, have different quadrupole splitting. The quadrupole splitting of the Mössbauer spectra ($\Delta E_Q = (1/2)|e|V_{zz}Q(1 + \eta^2/3)^{1/2}$) is directly related with the principal value (V_{zz}) of the electric field gradient tensor at the Fe nucleus. The principal value of the electric field gradient embraces contributions from both the valence electrons of the atom and from surrounding ions in the lattice. By taking these contributions separately we can write $V_{zz}/|e| = q = (1 - R)q_{\text{ion}} + (1 - \gamma_{\infty})q_{\text{latt}}$ where R and γ_{∞} represent the effects of shielding and antishielding respectively of the nucleus by the core electrons.^{17,18} For the high spin Fe^{3+} due to the spherical symmetry only the lattice contribution is significant. On the other hand, since the coordination octahedron of the Fe^{4+} ion is regular we claim that its valence contribution in V_{zz} is very low, thereby the observed quadrupole splitting mainly arises from the lattice part too. Consequently, it is reasonable for one to ask, why different quadrupole splitting for the two sites is observed. Of course, the iron as a local probe "sees" a statistical summation (not an averaging) of all possible spectra coming from the different configurations due to deficient Na site. A simple point charge calculation based on different configurations of sites Na(1) and Na(2) demonstrate that in such a case a broad quadrupole distribution is expected. Contrary to this we observed two distinct values of quadrupole splitting for each valence state. In order to explain this experimental fact we propose that a charge ordering which include the Co^{+3} and Co^{+4} and/or Na ions in Na(1) and Na(2) sites takes place producing, therefore, two distinct environments. A similar cobalt-charge and Na ordered configuration has also been proposed by Mukhamedshin et al.,⁶ Ning et al.,⁷ based on their NMR results and by Bernhard et al.⁸ by interpreting their ellipsometry data, for an $x = 3/4$ sample.

It is interesting to mention here the hyperfine parameters of the $\alpha\text{-NaFeO}_2$ compound¹⁹ which has similar crystal structure ($R\bar{3}m$) and the Fe is octahedrally coordinated with oxygen. At 4.2 K, NaFeO_2 displays a magnetically split Mössbauer spectrum with $H = 455$ kOe. At $T = 300$ K the Mössbauer spectrum consist of a doublet with $\delta = 0.33$ mm/s and $\Delta E_Q = 0.46$ mm/s. These values are very close to those of the second site, observed in AP $\text{Na}_{0.82}\text{CoO}_2$ compound, justifying the as-

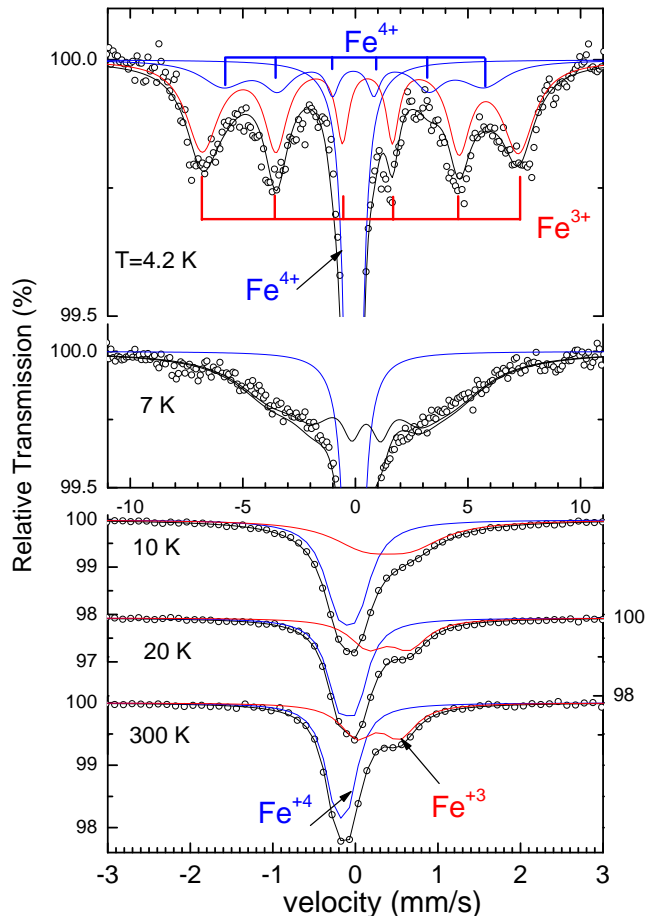


FIG. 5: Mössbauer spectra of AP $\text{Na}_{0.82}\text{CoO}_2$ (doped by 1% Fe-57) sample, at $T = 4.2, 7, 10, 20$ and 300 K.

TABLE I: Mössbauer parameters for AP $\text{Na}_{0.82}\text{CoO}_2$ at $T = 300$ K and 4.2 K. Half linewidth $\Gamma/2$ (mm/s), isomer shift δ relative to metallic Fe at RT (mm/s), hyperfine magnetic field H (kG), Quadrupole splitting $2\epsilon \equiv \Delta E_Q$, [$\epsilon = (1/4)|e|V_{zz}Q(1 + \eta^2/3)^{1/2}$, and $\epsilon = (|e|V_{zz}Q/8)(3\cos^2\Theta - 1 + \eta\sin^2\Theta\cos 2\Phi)$ for the paramagnetic, and the magnetic (first order perturbation theory) cases, respectively]. The numbers in parentheses are estimated standard deviations referring to the last significant digit.

	$T = 4.2$ K		
	SITE I(a) Fe^{4+}	SITE II Fe^{3+}	SITE I(b) Fe^{4+}
$\Gamma/2$	0.230(2)	0.24	0.16
δ	0.017(2)	0.484(5)	0.020(1)
ϵ	0.10(1)	-0.123(5)	0.01(5)
H	0	438(4)	356(8)
ΔH	0	37(3)	61(5)
Area	40(1)	43(1)	17(5)
	$T = 300$ K		
	SITE I	SITE II	
$\Gamma/2$	0.153(7)	0.24(1)	-
δ	-0.06(1)	0.38(1)	-
ϵ	0.09(1)	0.25(1)	-
Area	60(2)0	40(2)	-

signment to Fe^{3+} . Furthermore, deintercalated Na_xFeO_2 compound displays²⁰ two doublets, the first corresponding to Fe^{4+} and the second to Fe^{3+} . Contrary, however, to the $\text{Na}_{0.82}\text{CoO}_2$ compound the quadrupole splitting of the Fe^{4+} component is comparable with that of Fe^{3+} . This fact further supports our claim for cobalt-charge and Na ordering. Lowering the temperature, the Mössbauer spectra do not change down to 10 K with a constant area ratio of 60 : 40 for the Fe^{4+} and Fe^{3+} components respectively. At 10 K part of the spectrum is broadened and with further lowering of the temperature magnetic hyperfine splitting appears together with an unsplit peak, corresponding to the Fe^{4+} component (see Fig.5). The area ratio of these two components is inverted now to the value 40 : 60, a fact that leads us to conclude that the magnetic component arises from all the Fe^{3+} paramagnetic spectra area (40%) and part (20%) of the Fe^{4+} one. In view of this, we have least-squares fitted the 4.2 K spectrum with two magnetic components and one unresolved doublet. Both magnetically split components display inhomogeneous line broadening accounted for by the ΔH parameter which represents the full width at the half maximum of a Lorentzian distribution of the hyperfine magnetic field. This phenomenological parameter arises either from a static distribution of the electronic spin $\langle S \rangle$ or from spin fluctuation. Its value decreases with temperature for spectra taken between 10 K and 4.2 K indicating thus spin fluctuations. Such spin fluctuations can occur in isolated paramagnetic ions (paramagnetic spin relaxation) or in low dimension magnetically ordered systems, which is probably the case in the present structure. It is not clear to us why 2/3 of the Fe^{4+} component remains magnetically unsplit down to 4.2 K. We could speculate that the charge order model is not perfect and there are regions in the lattice that are disordered or different kind of ordering occurs.

Another characteristic of the hyperfine magnetic field value for the Fe^{3+} component is that it is lower than the expected for typical octahedral coordinated $\text{Fe}^{3+}\text{O}_6^{2-}$, ($S = 5/2$). The lower hyperfine field of Fe^{3+} component can be attributed either to covalency effects or to low dimensional effects. Recent NMR studies⁶ on a sample with $x = 0.66$ and our NMR results did not display any anomaly either in the linewidth or in the signal intensity, indicating that no magnetic transition occurs down to 1.5 K, in agreement with our magnetization measurements.

The Mössbauer spectra of the OP sample are similar with the AP sample with the exception of the area ratio of the two components that now became 65% to 35% indicating that part of the Fe^{3+} component was further oxidized to Fe^{4+} . Probably this is related with the two phase behavior revealed from our x-ray diffraction results for this particular sample. The 4.2 K magnetic spectra

were analyzed with the same model as for the AP sample and the analysis gave the same hyperfine parameters as for the AP sample. It is useful to compare the hyperfine parameters of the Fe^{4+} site with the Mössbauer parameters of the compound $\text{SrFe}^{4+}\text{O}_3$ containing iron in Fe^{4+} high spin state.²¹ This compound shows a single line at room temperature with an isomer shift of 0.054 mm/s and a magnetic hyperfine pattern at 4.2 K with an isomer shift 0.146 mm/s and a $H = 331$ kG. The H originates from an octahedral $d^4(t_{2g}^3e_g^1, S = 2)$ high-spin Fe^{4+} configuration with some degree of covalency, bearing in mind that $d^5(S = 5/2)$ high-spin Fe^{3+} ions can show flux densities as low as 450 kG. Comparing these hyperfine parameters with those of site (I), there is no doubt that this site corresponds to high spin ($S = 2$), Fe^{4+} .

Finally, it is necessary to compare our data with those of single crystals. The properties of samples Na_xCoO_2 ($x \sim 0.75$) are sensitive to the details of sample preparation. Polycrystalline powder and single crystals with the same nominal compositions exhibit qualitatively different properties. The single crystals prepared by the floating zone method exhibit an antiferromagnetic transition at 22 K, and a sharp first order transition at about 340 K.^{22,23} The powder shows no magnetic transition above 2 K and the first order transition at higher temperatures is smeared over the temperature range from 250 to 310 K as a series of first order transitions. The different properties between powder and single crystal samples is likely related to the real Na amount in the structure of Na_xCoO_2 and the distribution of Na in Na(1) and Na(2) sites. We would like to emphasize that despite the evidence for A-type antiferromagnetic correlations in $x \geq 0.75$ samples²⁴ a clear demonstration of the antiferromagnetism by means of a static magnetic order (elastic magnetic Bragg peaks) is still lacking. Possibly, this is the cause for the broad magnetically split Mössbauer spectra below $T \sim 7\text{K}$.

Summarizing we studied the $\text{Na}_{0.82}\text{CoO}_2$ (doped with 1% ^{57}Fe) using Mössbauer and NMR spectroscopies, dc magnetization measurements and x-ray diffraction data. The Mössbauer data clearly show that the deficient charge reservoir of Na-planes creates a mixed valance compound comprising from, Co^{3+} and Co^{4+} . Parts of the Mössbauer spectrum corresponding to Fe^{4+} and Fe^{3+} becomes magnetically split below 10 K. The magnetic spectra may imply a magnetic glass phase or slow electronic spin relaxation phenomena, because the magnetization measurements do not show any characteristic feature corresponding to a magnetic transition. The different quadrupole splitting of the two iron valence states indicate a charge ordered structure.

* Author to whom correspondence should be addressed.
email: mpissas@ims.demokritos.gr

¹ K. Takada, H. Sakurai, E. Takayama-Muromachi, F.

- Izumi, R. A. Dilanian and T. Sasaki, Nature (London) **422**, 53 (2003).
- ² J.-M. Tarascon and M. Armand, Nature (London) **414**, 359 (2001).
- ³ I. Terasaki, Y. Sasago and K. Uchinokura, Phys. Rev. B **56** R12685 (1997).
- ⁴ C. Fouassier, G. Matejka, J.-M. Reau and P. Hagenmuller, J. Solid State Chem. **6**, 532 (1973).
- ⁵ R. Ray, A. Ghoshray, K. Ghoshray S. Nakamura, Phys. Rev. B **59**, 9454 (1999).
- ⁶ I. R. Mukhamedshin, H. Alloul, G. Collin, and N. Blanchard, Phys. Rev. Lett. **93** 167601 (2004).
- ⁷ F.L. Ning, T. Imaia, B.W. Statt, and F.C. Choud, cond-mat/0408521 (unpublished).
- ⁸ C. Bernhard, A.V. Boris, N. N. Kovaleva, G. Khaliullin, A.V. Pimenov, Li Yu, D. P. Chen, C.T. Lin, and B. Keimer, Phys. Rev. Lett. **93**, 167003 (2004).
- ⁹ Q. Huang, J. W. Lynn, B. H. Toby, M.-L. Foo, and R. J. Cava, J. Phys.: Condens. Matter **16**, 5803 (2005).
- ¹⁰ J. L. Gavilano, D. Rau, B. Pedrini, J. Hinderer, H. R. Ott, S. M. Kazakov, and J. Karpinski, Phys. Rev. B **69**, 100404(R) (2004).
- ¹¹ T. Motohashi, R. Ueda, E. Naujalis, T. Tojo, I. Terasaki, T. Atake, M. Karppinen, and H. Yamauchi, Phys. Rev. B **67**, 064406 (2003).
- ¹² Takeo Tojo, Hitoshi Kawaji, Tooru Atake, Yasuhisa Yamamura, Masamichi Hashida, and Toshihide Tsuji, Phys. Rev. B **65**, 052105 (2002).
- ¹³ J. Rodríguez-Carvajal, Physica B **192**, 55 (1993).
- ¹⁴ R. J. Balsys and R. L. Davis, Solid State Ion. **93**, 279 (1996).
- ¹⁵ Q. Huang, M. L. Foo, R. A. Pascal, Jr., J. W. Lynn, B. H. Toby, Tao He, H. W. Zandbergen, and R. J. Cava, Phys. Rev. B **70**, 184110 (2004).
- ¹⁶ J.D. Jorgensen, M. Avdeev, D.G. Hinks, J.C. Burley, and S. Short, Phys. Rev. B **68**, 214517 (2003).
- ¹⁷ N. N. Greenwood, T. C. Gibb, *Mössbauer Spectroscopy*, (Chapman and Hall Ltd. 1971).
- ¹⁸ R. Ingalls, Phys. Rev. **133**, A787 (1964).
- ¹⁹ T. Ichida, T. Shinjo, Y. Bando and T. Takada, J. Phys. Soc. Japan **29**,795 (1970).
- ²⁰ Y. Takeda, K. Nakahara, M. Nishijima, N. Imanishi, O. Yamamoto, M. Takano, and R. Kanno, Mat. Res. Bull. **29**,659 (1994).
- ²¹ P. K. Gallagher, J. B. MacChesney, and D. N. E. Buchanan, J. of Chem. Phys. **41** , 2429 (1964).
- ²² B. C. Sales, R. Jin, K. A. Affholter, P. Khalifah, G. M. Veith, and D. Mandrus, Phys. Rev. B **70**, 174419 (2004).
- ²³ S. P. Bayrakci, C. Bernhard, D. P. Chen, B. Keimer, R. K. Kremer, P. Lemmens, C. T. Lin, C. Niedermayer, and J. Stremper Phys. Rev. B. **69**, 100410(R) (2004).
- ²⁴ S. P. Bayrakci, I. Mirebeau, P. Bourges, Y. Sidis, M. Enderle, J. Mesot, D. P. Chen, C. T. Lin, B. Keimer, cond-mat/0410224 (unpublished)